Beverage Plant Research

ARTICLE

Open Access

https://doi.org/10.48130/bpr-0024-0019

Beverage Plant Research **2024**, 4: e017

Neuroprotective comparisons and bioactive profiles of green tea and black tea: *in vitro* cellular experiments, metabolomics, and network pharmacology analysis

Huan Wu[1,2,3,4#], Juan Wan[1,2,3,4#], Jiayi Yuan[1,2,3,4], Mingwei Xie[1,2,3,4], Qing Nie[1,2,3,4], Zhonghua Liu[1,2,3,4*] and Shuxian Cai[1,2,3,4*]

[1] *National Research Center of Engineering Technology for Utilization of Botanical Functional Ingredients, Hunan Agricultural University, Changsha 410128, China*
[2] *Key Laboratory of Ministry of Education for Tea Science, Hunan Agricultural University, Changsha 410128, China*
[3] *Co-Innovation Center of Education Ministry for Utilization of Botanical Functional Ingredients, Hunan Agricultural University, Changsha 410128, China*
[4] *Key Laboratory for Evaluation and Utilization of Gene Resources of Horticultural Crops, Ministry of Agriculture and Rural Affairs of China, Hunan Agricultural University, Changsha, China*
[#] Authors contributed equally: Huan Wu, Juan Wan
* Corresponding authors, E-mail: zhonghua-liu@hunau.edu.cn; caishuxian@hunau.edu.cn

Abstract

This study aimed to compare the neuroprotective effects of green tea and black tea, made from the same raw materials, on an A$\beta_{25\text{-}35}$-induced PC12 cell model, using Ultra-High Performance Liquid Chromatography-Tandem Mass Spectrometry (UPLC-MS/MS) and network pharmacology approaches. This addresses the gap in current research, which has extensively explored the neuroprotective properties of green tea and its components but has paid less attention to black tea. The findings indicate that both teas can alleviate Aβ-induced neurodegenerative changes by reducing inflammation, mitochondrial disruption, and other cellular stressors. Notably, black tea showed higher effectiveness, enriching more differentially expressed genes within critical pathways and exhibiting a broader spectrum of bioactive compounds. Its protein-protein interaction network also suggested that black tea acted on a wider range of potential targets. However, these results are preliminary and emphasize the importance of the complex interplay of bioactive components in tea, advocating for further comparative studies to fully understand their neuroprotective mechanisms.

Citation: Wu H, Wan J, Yuan J, Xie M, Nie Q, et al. 2024. Neuroprotective comparisons and bioactive profiles of green tea and black tea: *in vitro* cellular experiments, metabolomics, and network pharmacology analysis. *Beverage Plant Research* 4: e017 https://doi.org/10.48130/bpr-0024-0019

Introduction

Increasing evidence suggests the imbalance between the accumulation and clearance of amyloid β (Aβ) and Aβ-related peptides plays a crucial role in the onset of Alzheimer's disease (AD)[1,2]. Aβ is known to trigger various stress responses, including oxidative stress, inflammation, and mitochondrial dysfunction[3–5]. Externally, Aβ forms senile plaques outside of cells, while intracellular hyperphosphorylated tau protein forms neurofibrillary tangles and cell apoptosis, both of which are important factors leading to the development and progression of AD[6–8].

Moreover, Aβ exerts multiple toxic effects, such as causing ion leakage, disruption of cellular calcium ion balance, and induction of cell apoptosis[9]. Beyond external accumulation, Aβ can also accumulate in cell membranes, organelles, and the cell nucleus, leading to mitochondrial dysfunction, endoplasmic reticulum stress, and abnormal cell cycle[10,11]. This buildup triggers microglia activation, leading to the production and release of pro-inflammatory cytokines, including IL-6 and TNF-α[12]. Additionally, Aβ can stimulate the reactivation of the mitotic cycle in neurons, hastening their apoptosis[13].

Numerous investigations have indicated that tea and its functional components can delay brain aging[10,14–18]. Key active ingredients in green tea, such as catechins and theanine, are noted for their ability to prevent the accumulation of Aβ aggregates, while also providing anti-inflammatory, antioxidant, and axonal growth stimulation[16,19–22]. Black tea accounts for approximately 80% of the world's tea production and has the quality characteristics of 'red tea, red soup, red leaves, and mellow taste'[23]. Research has found that black tea can inhibit the formation of Aβ aggregates and has significant protective effects against Aβ-induced neurotoxicity[24]. In a rat model of attention deficit hyperactivity disorder (ADHD), black tea has been shown to effectively counteract Aβ-induced neurotoxicity and prevent memory loss[10,25,26]. The exact mechanisms behind black tea's protective effects in the brain remain to be fully elucidated.

This research established a neurodegeneration model of Alzheimer's disease (AD) using PC12 cells exposed to A$\beta_{25\text{-}35}$ to compare the effectiveness of green tea and black teas, derived from the same batch of leaves, in mitigating Aβ-induced cellular dysfunction. Furthermore, this study employed a comprehensive metabolomic analysis of tea components, alongside network pharmacology approaches, to explore the neuroprotective qualities of both green tea and black tea.

Materials and methods

Reagents and materials

The tea raw materials used in the experiment were commercially available green tea and black tea. Fresh tea leaves of the same variety and from the same period of time were used to make the tea. 3-(4,5-Dimethyl-2-Thiazolyl)-2,5-Diphenyl Tetrazolium Bromide (MTT), and Dimethyl sulfoxide (DMSO) were purchased from Sigma-Aldrich (St Louis, MO, USA). RIPA lysate, protease inhibitor mixture, and anti-fluorescence quenching agent (containing DAPI) were purchased from Beyotime Biotechnology (Shanghai, China). In addition to anti-GAPDH, anti-IL-6, anti-NF-κB, anti-Histone H3, anti-Sirt1, anti-Cyclin B1, anti-Cyclin D1, anti-Bax, anti-Bcl-2 and anti-AMPK (Cell Signaling, Boston, MA, USA), the following primary antibodies were also used for Western blot analysis: anti-multiubiquitin (UPs) (Medical & Biological Laboratories co. Ltd, Tokyo, Japan), anti-4-HNE (Millipore, Boston, USA), anti-sequestosome-1 (p62) (Epitomics, Burlingame, CA, USA), anti-Klotho (Novusbio, Littleton, USA) and anti-RAGE (Santa Cruz Biotechnology, Dallas, TX, USA). Rabbit anti-Goat IgG-HRP Antibody, Goat anti-Rabbit IgG-HRP Antibody, Goat anti-Mouse IgG-HRP Antibody were purchased from Absin Biotechnology (Shanghai, China). Western chemiluminescent horseradish peroxidase substrate was purchased from Millipore (Boston, USA).

Preparation of tea water extract

To accurately simulate the neuroprotective effects of tea consumption, this study utilized a simulated tea brewing method and a direct freeze-drying process to accurately preserve the components and particle structures of the tea infusion. Specifically, 100 g each of green tea and black tea were accurately weighed and placed into conical flasks containing 1 L of boiling water (100 °C), followed by a 45-min immersion in a 100 °C water bath, filtered, and then subjected to another liter of boiling water for an additional 45 min in the water bath. The infusions from each tea were combined, cooled to room temperature, pre-frozen at −20 °C for 24 h, and freeze-dried to produce green tea and black tea water extracts, subsequently stored at −20 °C.

Preparation of A$\beta_{25\text{-}35}$ with different treatments

A$\beta_{25\text{-}35}$ (1 mM), A$\beta_{25\text{-}35}$ (1 mM)/green tea (1 mM) and A$\beta_{25\text{-}35}$ (1 mM)/black tea (1 mM) were preincubation in sterile water for 7 d in a constant temperature incubator at 37 °C to obtain A$\beta_{25\text{-}35}$, A$\beta_{25\text{-}35}$/green tea, A$\beta_{25\text{-}35}$/black tea proteins.

ThT signal detection

Thioflavin T (ThT) was used to analyze the β-sheet structure generated during amyloid aggregation[25]. A$\beta_{25\text{-}35}$ (50 μM), A$\beta_{25\text{-}35}$ (50 μM)/green tea (50 μg/mL) and A$\beta_{25\text{-}35}$ (50 μM)/black Tea (50 μg/mL) were incubated at 37 °C for 7 d. In subsequent experiments, these groups of proteins were abbreviated as A$\beta_{25\text{-}35}$, A$\beta_{25\text{-}35}$/green tea and A$\beta_{25\text{-}35}$/black tea, respectively. ThT was assayed as follows: 40 μL of different protein solutions and 160 μL of ThT working solution were aspirated in a 96-well plate. The fluorescence intensity was measured on a multifunctional microplate apparatus at an excitation wavelength of 440 nm and an emission wavelength of 485 nm.

Cell culture and drug treatment

PC12 cells were inoculated at 1×10^5/mL in a culture dish containing DMEM medium with 10% FBS and incubated in a constant temperature incubator at 37 °C containing 5% CO_2. The medium was changed every 2 d, and when the cells reached 60%–70% fusion rate, the cells were treated with A$\beta_{25\text{-}35}$, A$\beta_{25\text{-}35}$/green tea, and A$\beta_{25\text{-}35}$/black tea for 24 h. For the control group (Control) cells, equal amounts of sterile water were added.

Cell viability

PC12 cells were seeded at 1×10^4 cells/well in a 96-well plate and cultured for 24 h. Cells were incubated with the different protein samples (A$\beta_{25\text{-}35}$, A$\beta_{25\text{-}35}$/green tea, A$\beta_{25\text{-}35}$/black tea) prepared as above and the control group was added with the same amount of sterile water. After 24 h, the cell viability of different treatment groups was detected using the MTT method[26].

ATP detection

Cells were inoculated in 6-well culture plates at 1.5×10^5 cells/well and cultured as described above. Then the supernatant was aspirated, the cells were washed twice by adding pre-cooled PBS, and 200 μL of lysate was added, and the supernatant was collected by centrifugation (4 °C, 12,000 rpm, 5 min) to determine the ATP content (Beyotime Biotechnology, Shanghai, China).

Detection of reactive oxygen species (ROS)

Cells were inoculated in 6-well culture plates at a density of 1.5×10^5 cells/well, and cell culture was performed as described above. The cells were collected and suspended in diluted DCFH-DA (10 μM) and incubated in a cell culture incubator at 37 °C for 20 min. The cells were washed three times with a serum-free cell culture medium to remove the DCFH-DA that had not entered the cells fully. Then, the fluorescence values were detected at 488 nm excitation wavelength and 525 nm emission wavelength using a fluorescence zymograph.

JC-1 fluorescent staining

Cells were inoculated at a density of 5×10^4 cells/well onto cell crawls in 24-well culture plates, and cell culture was performed as described above. The supernatant was then aspirated and the cells were washed twice by adding pre-cooled PBS. Cell culture medium (250 μL) was added to each well, then 250 μL of JC-1 staining working solution was added to each well and incubated in a cell incubator at 37 °C for 20 min. 300 μL of JC-1 staining buffer (1×) was added to wash the cells twice, followed by blocking the slides with an anti-fluorescent bursting agent (containing DAPI). Images were acquired using a fluorescence microscope (Zeiss, Axio scope. A1). The average fluorescence intensity of the images was measured using ZEN software package. Three measurements were taken, each time measuring an area of the same size.

BODIPY fluorescent staining

Cellular lipid droplet staining was performed using the BODIPY fluorescent probe (Invitrogen, New York, USA). Cells were treated according to the methods described above. After the experiment, the cells were collected and stained strictly following the kit's instructions. Finally, photographs were taken with a fluorescence microscope (Zeiss, Axio scope. A1), and the average fluorescence intensities of different treatment groups were calculated using ZEN software.

Western blotting analysis

Cells were inoculated at 6×10^5 cells/well in a 10 cm diameter cell culture dish, and cell culture was performed as

described above. The supernatant was then aspirated, cells were washed twice by adding pre-cooled PBS, and 500 μL of RIPA lysate containing protease inhibitors and the supernatant was collected by centrifugation (4 °C, 12,000 rpm, 20 min). The protein concentration was determined by the BCA protein analysis kit (Pierce, Grand Island, NY, USA). Equal amounts of protein from each sample were separated on 8%–10% SDS-PAGE gels. Proteins from the gels were transferred to PVDF (Millipore, USA) membranes. The membranes were closed in TBST buffer containing 5% skim milk powder for 1 h. The membranes were then incubated overnight at 4 °C in the primary antibody at dilution ratios of 1:500–1:2000. After washing in TBST buffer, the membranes were incubated with appropriate secondary antibodies for 90 min at room temperature. Signals were detected using enhanced chemiluminescence (ECL) detection kit (Millipore, USA) and analyzed by Western blot densitometry using Image-J software[26].

ELISA kit detection

ELISA detection kits (Jiangsu Feiya Biotechnology, Yancheng, China) were used to determine the contents of GAP43 and TNF-α in the protein samples of different treatment groups prepared above.

Transcriptome analysis

Cell experiments were performed according to the methods above. After the experiment, the collected cell samples were snap-frozen in liquid nitrogen, frozen in dry ice, and sent to BGI Company (Shenzhen, China) for subsequent RNA-seq detection (BGISEQ-500 sequencer). In order to explore molecular pathways and networks more comprehensively from the transcriptome level, a sufficient number of differential genes (DEGs) were screened with $|\text{fold change}| \geq 1.2$ and $Q \leq 0.05$ for heatmap, KEGG and gene interaction analysis. All analyses were performed using the online bioinformatics platform Dr. Tom (biosys.bgi.com/) provided by BGI.

Untargeted metabolomics of green tea and black tea

Pre-treatment, extract analysis, metabolite identification and quantification of green tea and black tea samples were performed at BGI-Shenzhen (Shenzhen, China) according to their standard procedures. Untargeted Metabolomics analysis was performed by UPLC-MS/MS technique using a high-resolution mass spectrometer Q Exactive HF (Thermo Fisher Scientific, USA) with separate data acquisition in both positive and negative ion modes to improve metabolite coverage. The VIP values of the first two principal components were modelled using Partial Least Squares Method-Discriminant Analysis (PLS-DA), and the results of Fold change and Student's t test obtained from univariate analysis were combined to screen for differential metabolites.

Network pharmacology

The screened compounds were converted into the Standard Simplified Molecular Input Line Entry System (SMILES) by Pubchem (https://pubchem.ncbi.nlm.nih.gov/) and screened for drug similarity by blood-brain barrier (BBB) permeation and SwissADME calculations (www.swissadme.ch), active compounds with a BBB of 'yes' and Bioavailability Score > 0.17 are considered to have good bioavailability. Probability > 0 was used as the screening threshold, pharmacological targets were obtained using the SwissTargetPrediction database. In the GeneCard database (www.genecards.org), the disease genes of 'Neurodegenerative changes' were searched for intersection targets for subsequent analysis. The Venn diagram was used to evaluate the potential targets of the intersection genes of green tea and black tea with neurodegenerative changes. GO and KEGG analysis of cross-targeted genes using the 'custom analysis' module in Metascape (https://metascape.org/gp/index.html), with species set to *Homo sapiens* and omicstudio (www.omicstudio.cn) visualized KEGG analysis of target genes. PPI analysis of targets was performed by STRING database (https://string-db.org/), with the target species set to *Homo sapiens* and a confidence level greater than 0.09. Then, the PPI network was visualized using Cytoscape software (version 3.9.1), with images showing only the core targets with degree values greater than the mean or above.

Statistical analysis

Statistical analysis was performed using the GraphPad Prism 8.01 software package. Combined with Turkey's multiple comparison test, one-way ANOVA was used to test the significance of differences, and the results were expressed as the mean ± standard deviation. $p < 0.05$ was significant, and $p < 0.01$ was judged to be extremely significant.

Results and analyses

Metabolomics analysis

UPLC-MS/MS technology was utilized for untargeted metabolomics analysis, with data acquisition in both positive and negative ionization modes to enhance the range of detected metabolites. The base peak ion chromatograms revealed that the total ion current (TIC) profiles for metabolite identification overlapped significantly, demonstrating consistent retention times and peak intensities, which suggests reliable instrument signal stability (Fig. 1a & b). Partial least squares-discriminant analysis (PLS-DA) showed that samples of green and black tea were distinctly separated within the 95% confidence interval ellipse, effectively differentiating between the two tea varieties based on their component qualities (Fig. 1c). Utilizing criteria such as a VIP score ≥ 1, a Fold-Change range of $0.83 \leq \text{Fold-Change} \leq 1.2$, and a q-value < 0.05, a total of 753 differential metabolites were screened. Among these, black tea demonstrated an increase in 570 metabolites and a decrease in 183 metabolites when compared to green tea (Fig. 1e). A heatmap further illustrated the propertional differences in various components between green tea and black tea (Fig. 1d).

Green tea and black tea inhibit A$\beta_{25\text{-}35}$-induced degenerative changes in differentiated PC12 cells

Research has shown that the formation of β-sheet structures plays a pivotal role in the early stages of amyloidgenesis[27,28]. Fluorescence detection revealed that the fluorescence intensity of A$\beta_{25\text{-}35}$ was about sevenfold higher than that of the control ($p < 0.01$), suggesting a significant increase in β-sheet structures within the A$\beta_{25\text{-}35}$ group. Treatment with both green tea and black tea markedly reduced the formation of these β-sheet structures ($p < 0.01$) (Fig. 2a). For simplicity, in the subsequent sections of the article, the treatments with A$\beta_{25\text{-}35}$ (50 μM), A$\beta_{25\text{-}35}$ (50 μM) combined with green tea (50 μg/ml), and A$\beta_{25\text{-}35}$ (50 μM) combined with black tea (50 μg/ml) are referred to as A$\beta_{25\text{-}35}$, A$\beta_{25\text{-}35}$/green tea and A$\beta_{25\text{-}35}$/black tea, respectively.

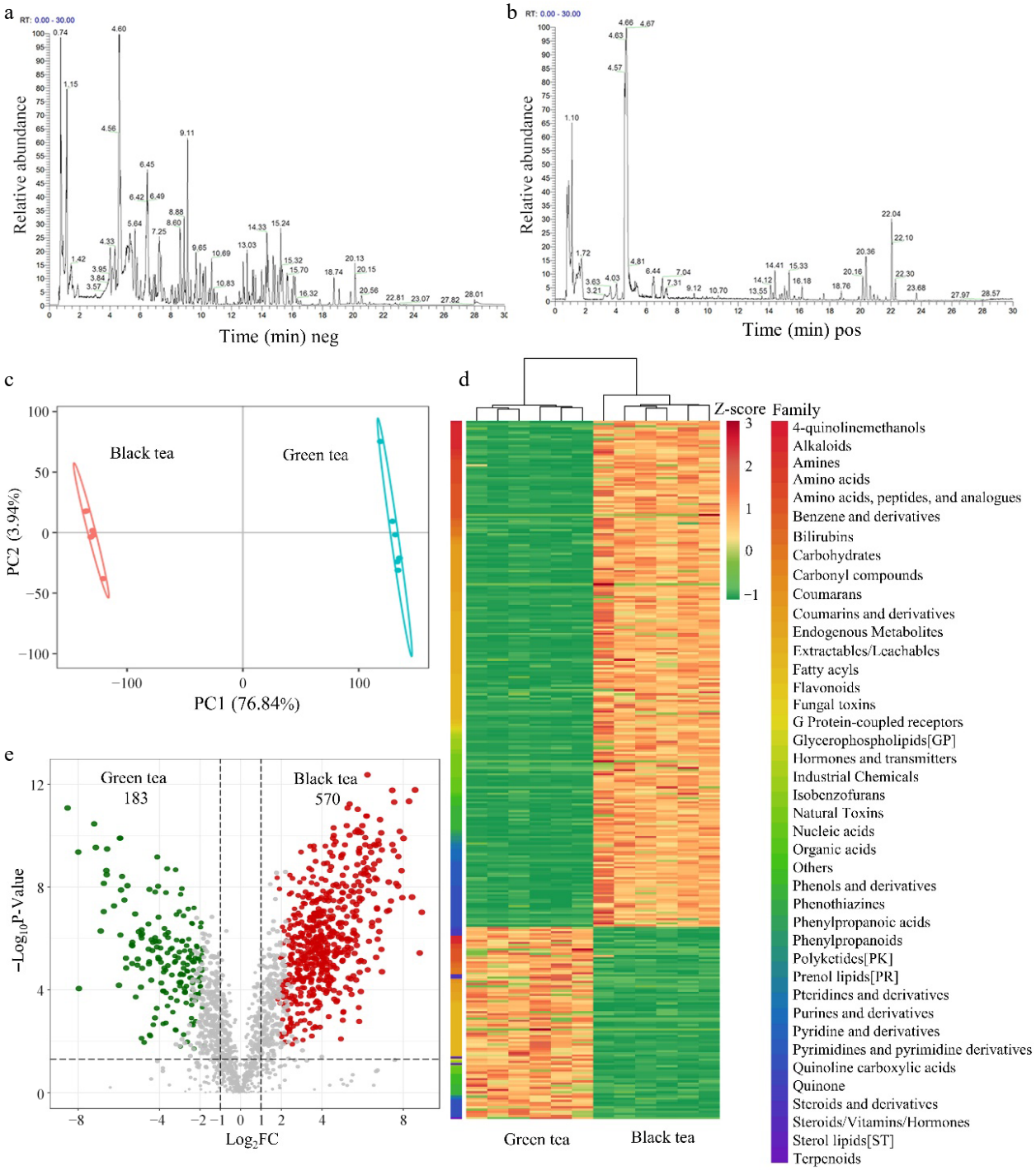

Fig. 1 Untargeted metabolomics analysis of aqueous extracts of green tea and black tea. (a), (b) Base peak ion chromatogram (BPC). (c) PLSDA Score Chart. (d) Heat map of differential metabolite clustering. Classification of compounds according to 'Family'. (e) Differential metabolite volcano map, VIP ≥ 1, 0.83 ≤ Fold-change of Difference ≤ 1.2, q-value < 0.05.

When well-differentiated PC12 cells were exposed to the various A$\beta_{25\text{-}35}$ samples for 24 h, the viability of cells treated with A$\beta_{25\text{-}35}$ alone decreased significantly ($p < 0.01$), as evidenced by enhanced DAPI staining and observations of fragmented or enlarged nuclei, indicating DNA damage. Conversely, green tea and black tea treatments significantly mitigated the toxicity induced by A$\beta_{25\text{-}35}$. Notably, cell viability in the A$\beta_{25\text{-}35}$/black tea group improved ($p < 0.01$), with DAPI staining results comparable to those of the control group (Fig. 2b & c).

The expression of GAP43 in neurons plays a pivotal role in axon elongation, synapse formation, and neural germination during development[29]. Bax and Bcl-2 are homologous water-soluble related proteins, and overexpression of Bax antagonizes the protective effect of Bcl-2, leading to cell death[30]. Cyclin B1 drives the G2/M phase transition, and Cyclin D1

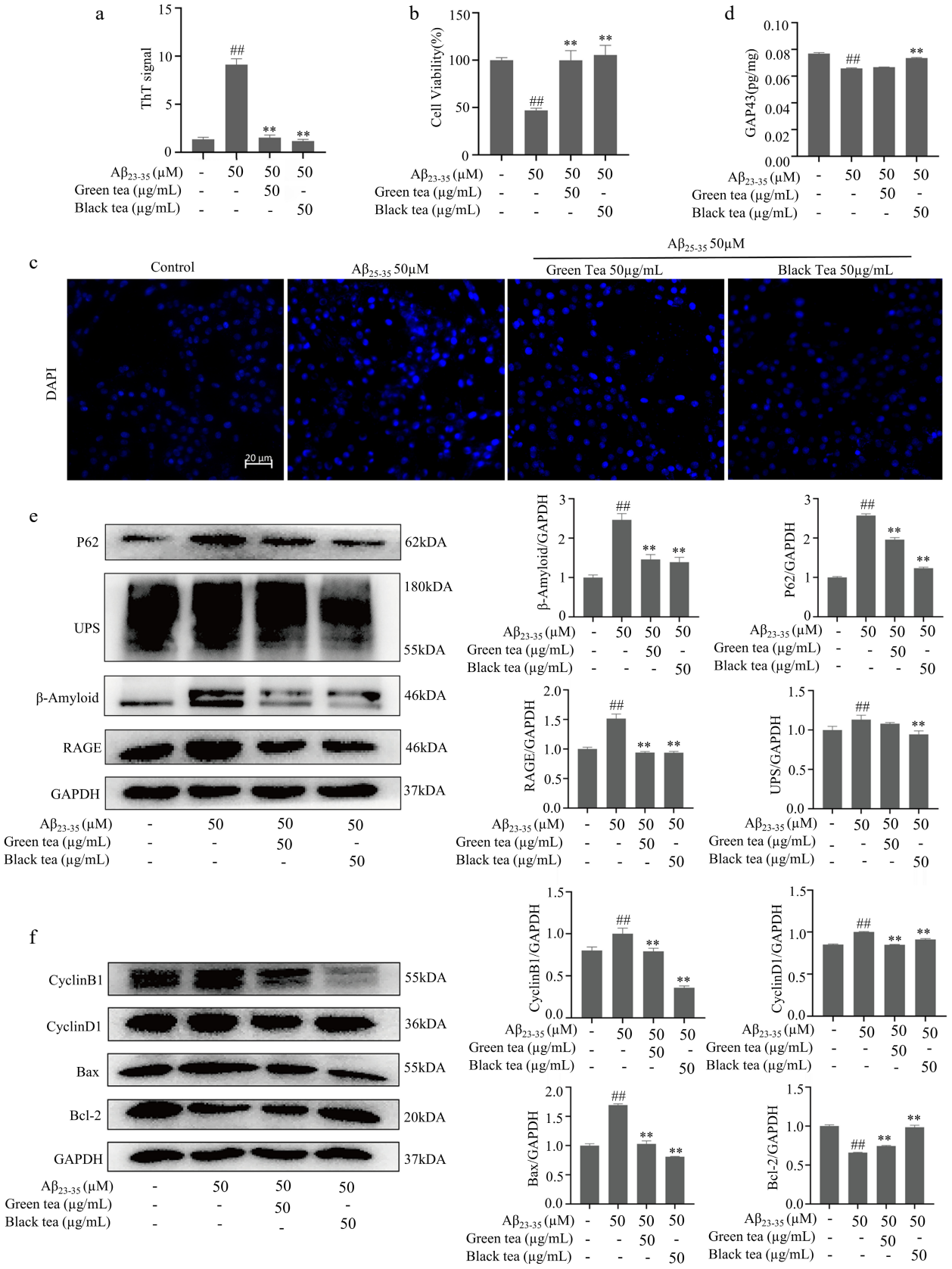

Fig. 2 Green tea and black tea inhibits A$\beta_{25\text{-}35}$-induced degenerative changes in differentiated PC12 cells. (a) ThT assay for β-fold structure content of different A$\beta_{25\text{-}35}$ incubated samples. (b) MTT assay for cell viability. (c) DAPI fluorescence staining (bar = 20 μm). (d) ELISA assay for GAP43 protein expression level. (e) Westen-blotting for Aβ and other protein aggregate-related pathways. (f) Westen-blotting detection of cell cycle and apoptosis-related pathways. Compared with the Control group, # $p < 0.05$, ## $p < 0.01$. Compared with A$\beta_{25\text{-}35}$ group, ** $p < 0.01$, n = 3.

regulates the G1/S phase transition, both key cell cycle regulators[31]. ELISA and Western blot analyses (Fig. 2d–f) revealed that in the A$\beta_{25\text{-}35}$-treated cells, the levels of GAP43 and Bcl-2 were significantly reduced ($p < 0.01$), whereas the levels of Bax, p62, UPs, β-Amyloid, RAGE, Cyclin B1 and Cyclin D1 were significantly elevated ($p < 0.05$ or $p < 0.01$). Conversely, these proteins exhibited reverse expression patterns in A$\beta_{25\text{-}35}$/black tea group cells. The findings suggest that A$\beta_{25\text{-}35}$ contributes to axonal atrophy, apoptosis, and the accumulation of toxic aggregates, thereby leading to aberrant cell cycle activation. Black tea exhibited a notable protective effect against the toxic stress induced by A$\beta_{25\text{-}35}$, performing better than green tea in this regard.

Anti-inflammatory and metabolism properties of green tea and black tea

Axons are rich in mitochondria, and mitochondrial dysfunction leads to neuronal axonal degeneration, the root cause of neurodegenerative diseases[32–34]. In cells treated with A$\beta_{25\text{-}35}$, there was a significant reduction in mitochondrial membrane potential (MMP) and ATP levels ($p < 0.01$), accompanied by an increase in ROS ($p < 0.01$) (Fig. 3a–d). Further, ELISA and Western blot assays showed that A$\beta_{25\text{-}35}$ promoted the nuclear translocation of NF-κB ($p < 0.01$), elevated the levels of TNF-α ($p < 0.01$), and decreased AMPK and Sirt1 protein levels ($p < 0.01$) (Fig. 3e & f). BODIPY staining for lipid droplets demonstrated that A$\beta_{25\text{-}35}$ treatment led to increased cellular lipid deposition ($p < 0.01$) (Fig. 3g & h). These findings imply that A$\beta_{25\text{-}35}$ triggers inflammatory pathways and suppresses cellular metabolism. Black tea exhibited a notable protective effect against mitochondrial damage, reduced inflammation and lipid accumulation, and enhanced cellular metabolic functions ($p < 0.01$), outperforming green tea in these respects.

Green tea and black tea mitigate neurodegeneration at the transcriptomic level

In comparison to the A$\beta_{25\text{-}35}$ group, the DEGs in both the A$\beta_{25\text{-}35}$/green tea and the A$\beta_{25\text{-}35}$/black tea groups were significantly increased, with the DEGs in the A$\beta_{25\text{-}35}$/black group being approximately 2.9 times higher than those in the A$\beta_{25\text{-}35}$ group (Fig. 4a). KEGG pathway analysis revealed that these DEGs were predominantly involved in processes such as ribosomes function, related neurodegeneration, oxidative phosphorylation, AGE-RAGE signaling pathway, RNA transport, and DNA replication, among others (Fig. 4b–d).

Heatmap and protein-protein interaction network (PPI) analysis of DEGs in different treatment groups with DEGs of A$\beta_{25\text{-}35}$/black tea as a reference. The expression patterns of DEGs in the tea-treated groups counteracted those observed in the A$\beta_{25\text{-}35}$ group. Specifically, the DEGs in the A$\beta_{25\text{-}35}$/black tea group predominantly enhanced pathways related to signal transduction, cell growth, and regeneration, while suppressing pathways associated with neurodegeneration, translation, transcription, protein folding, sorting and degradation, as well as networks related to endocrine and metabolic diseases. Moreover, black tea's impact on the transcriptome was more pronounced than that of green tea (Fig. 4e).

Exploring the neuroprotective active compounds of green tea and black tea through network pharmacology

To uncover the neuroprotective mechanisms of green tea and black tea on highly differentiated neuronal cells, network pharmacology approaches were employed to identify potential targets and pathways. Utilizing ADME (Absorption, Distribution, Metabolism, and Excretion) criteria, specifically a Bioavailability Score greater than 0.17, 46 active components in green tea and 155 in black tea that were upregulated were identified. Among these, 66 compounds from black tea and 14 from green tea were predicted to cross the blood-brain barrier (detailed compound information is provided in Supplemental Tables S1 & S2). The investigation highlighted 389 potential targets for green tea and 455 for black tea in combating neurodegenerative changes. GO (Gene Ontology) enrichment analysis revealed that both green tea and black tea target processes related to phosphorylation and protein kinase activity. Notably, green tea was associated with phosphotransferase activity, and alcohol group as acceptor, whereas black tea was linked to protein phosphorylation (Fig. 5a & b). KEGG analysis showed that the potential targets of both teas significantly impacted pathways involving neuroactive ligand-receptor interaction, cancer, PI3K-Akt signaling pathway, lipid and atherosclerosis, and MAPK signaling pathway. Despite the similarity in targeted pathways, black tea was found to enrich a greater number of genes within these pathways compared to green tea (Fig. 5c& d).

The analysis of active component-target interaction maps revealed that green tea combats neurodegenerative changes through key components such as benzene and its derivatives, endogenous metabolites, nucleic acids, amino acids, alkaloids, coumarins, terpenoids. Black tea, while encompassing these types of components, also includes organic acids, lipids, phenolic acids, and flavonoids, offering a wider and more varied spectrum of neuroprotective targets. Black tea stands out with 113 main differential active compounds, compared to green tea's 77, showcasing a greater diversity through higher compound interconnectivity. This suggests that black tea exhibits more complex biological activities (Fig. 6) (details of the compounds are provided in Supplemental Tables S3 & S4). SRC, identified as a pivotal target of black tea, is integral to central nervous system development and prevalent in neurons, highlighting black tea's nuanced neuroprotective capabilities[35].

Discussion

This research indicates that both green tea and black tea share similar protective mechanisms against A$\beta_{25\text{-}35}$-induced neurodegenerative changes in PC12 cells. Yet, black tea outperforms green tea in safeguarding mitochondria, preventing DNA damage, reducing lipid accumulation, and hindering the formation of aggregates (Figs 2 & 3). Further, transcriptomic analysis and network pharmacology studies suggest that black tea impacts a wider and more complex network of transcriptome and cellular signaling pathways, showcasing a richer array of bioactive compounds indicating a greater variety of bioactive components (Figs 4& 6).

Aβ's multiple toxic effects on neurons include inducing apoptosis, which contributes to neuronal loss[36]; and mitochondrial accumulation, which disrupts normal function[37]. These findings align with our study's outcomes. Black tea pre-incubation can attenuate A$\beta_{25\text{-}35}$-induced apoptosis of PC12 cells, enhance cell viability, and downregulate the expression of apoptotic pathway-related proteins (Fig. 2f). Mitochondrial dysfunction plays a key role in aging-related neurodegenerative diseases[38]. Aβ can impair neuronal function by damaging

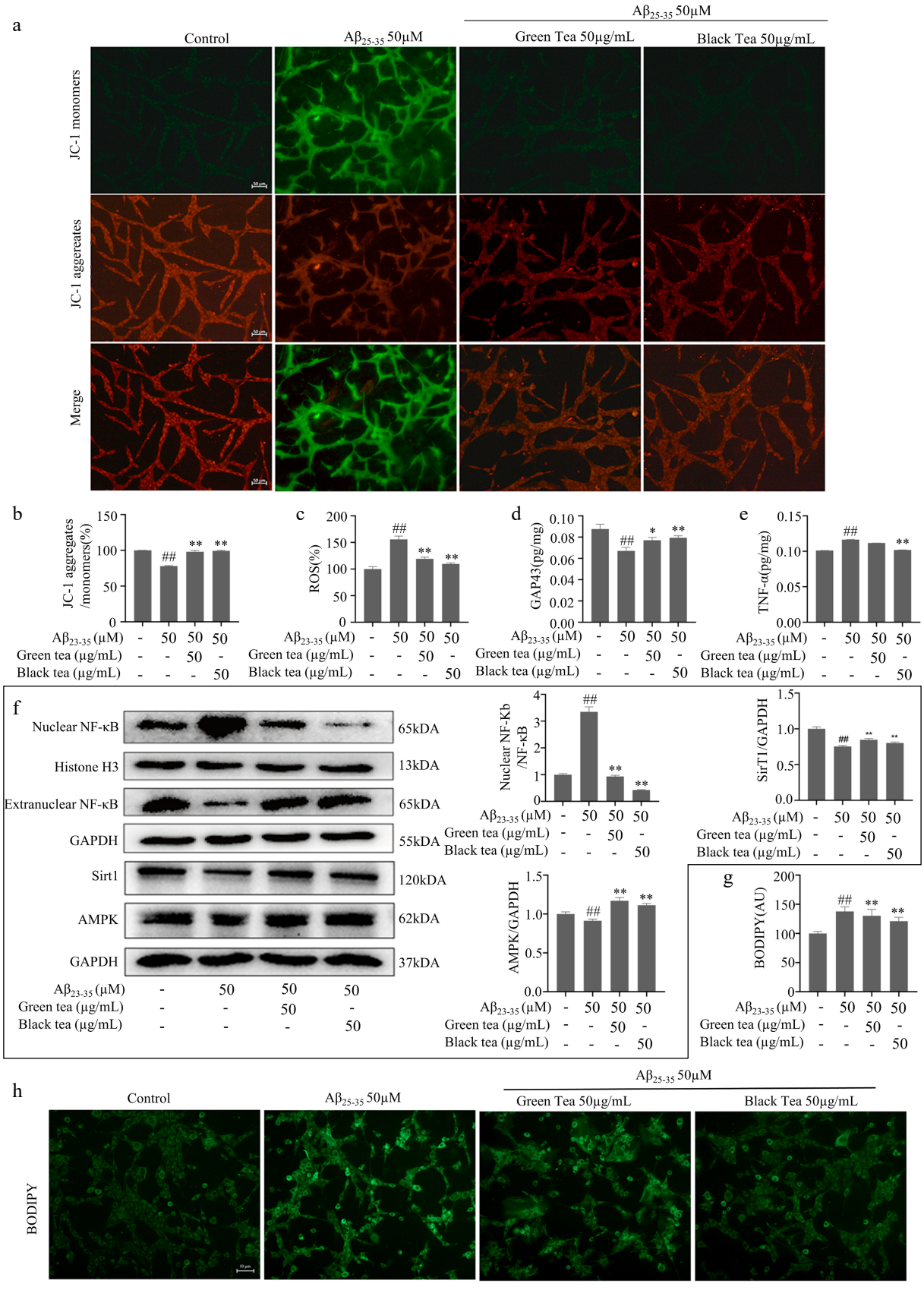

Fig. 3 Anti-inflammatory and metabolism-promoting functions of green tea and black tea. (a), (b) JC-1 staining plot with statistics (bar = 50 μm). (c) Fluorescence enzyme marker for ROS level. (d) ATP content assay. (e) ELISA for cellular TNF-α protein expression level. (f) Western-blotting for inflammation and energy metabolism-related pathways. (g), (h) BODIPY fluorescence staining with statistics for lipid droplets (bar = 10 μm). Compared with the Control group, ## $p < 0.01$; Compared with the A$\beta_{25\text{-}35}$ group, * $p < 0.05$, ** $p < 0.01$, n = 3.

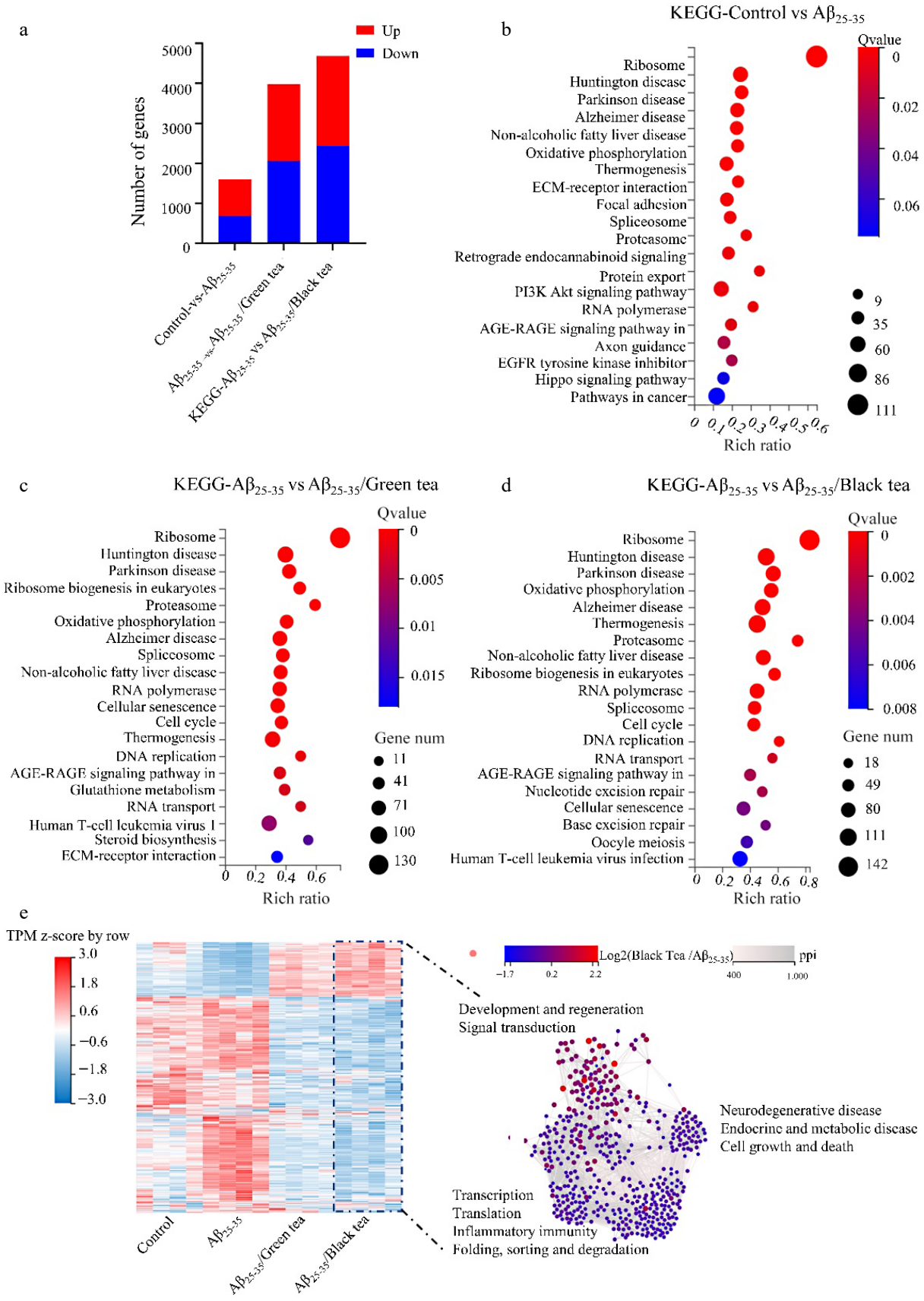

Fig. 4 Transcriptome analysis of different treatment groups. (a) Comparative analysis of DEGs between groups. (b)–(d) KEGG analysis of DEGs in different treatment groups. (e) Heatmap and interaction network analysis of DEGs in different treatment groups with DEGs of A$\beta_{25\text{-}35}$/black tea as a reference.

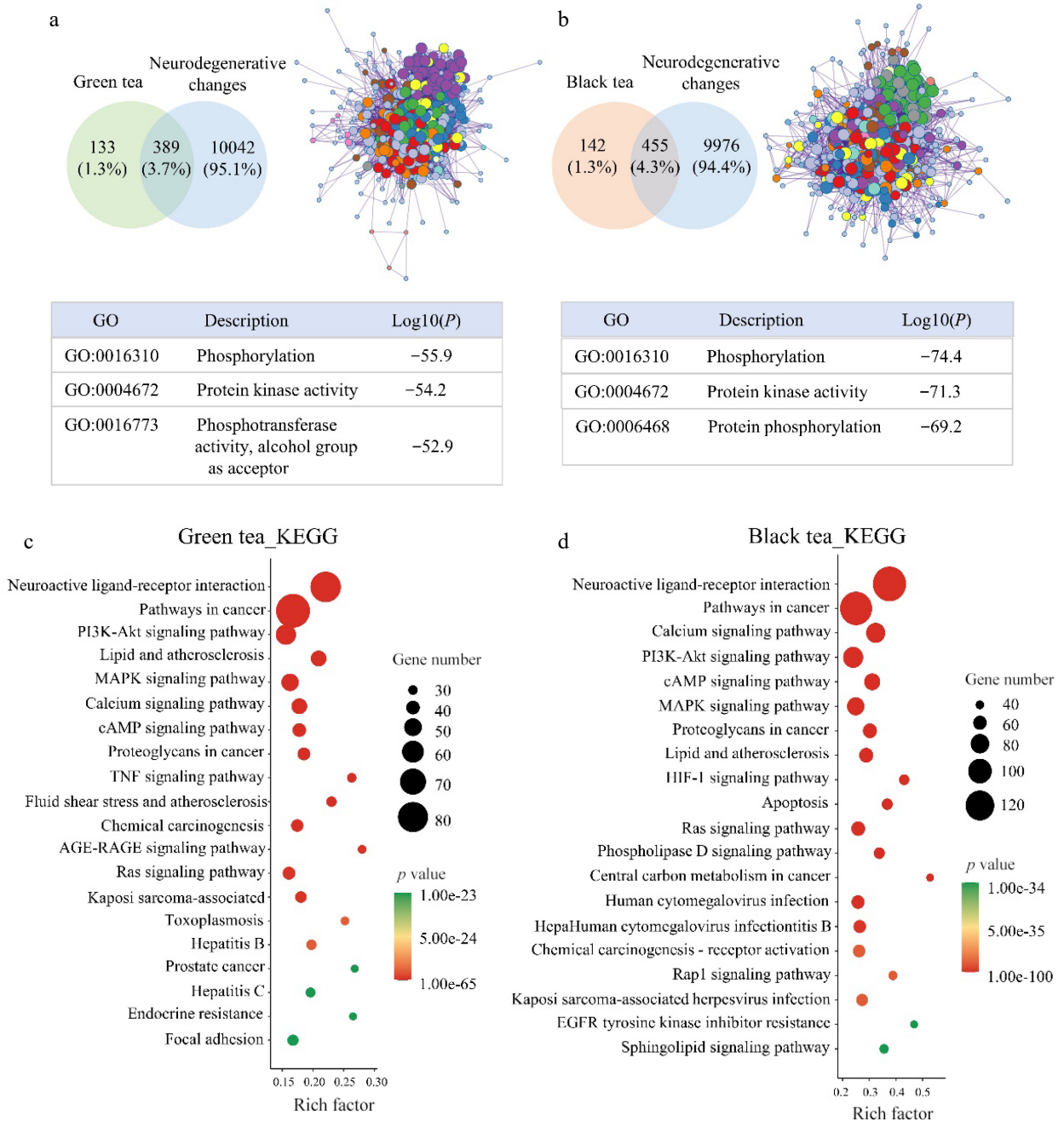

GO	Description	Log10(*P*)
GO:0016310	Phosphorylation	−55.9
GO:0004672	Protein kinase activity	−54.2
GO:0016773	Phosphotransferase activity, alcohol group as acceptor	−52.9

GO	Description	Log10(*P*)
GO:0016310	Phosphorylation	−74.4
GO:0004672	Protein kinase activity	−71.3
GO:0006468	Protein phosphorylation	−69.2

Fig. 5 Network pharmacological analysis of green tea and black tea against neurodegenerative changes. (a), (b) VENN and GO analysis. (c), (d) KEGG analysis.

mitochondrial electron transport chains and inhibiting ATP production[39]. Our findings show that the pre-incubation with black tea significantly restores mitochondrial membrane potential, increases ATP levels, and elevates the expression of proteins in energy-metabolism pathways (Fig. 3a, d–f). For highly differentiated cells to undergo normal differentiation and maintain physiological functions, they must remain in a stationary phase of their cycle. Promoting axonal differentiation has been identified as crucial in combating neurodegenerative diseases[40]. Black tea appears to prevent neuronal degeneration by enforcing cycle arrest, outperforming green tea in this regard and aligning with previous research findings.

Oxidative stress induced by Aβ leads to the oxidation of polyunsaturated fatty acids (PUFAs) in cell membranes through free radical chain reactions, resulting in the formation of lipid hydroperoxides such as 4-HNE[41]. These lipid hydroperoxides, including 4-HNE, can bind to nucleophilic functional groups in proteins, nucleic acids, and membrane lipids, thereby contributing to the impairment of autophagy[41]. When autophagy is disrupted, protein aggregates and damaged organelles accumulate within cells[42,43], leading to the cellular buildup of p62 and ubiquitin-modified proteins[44,45]. Black tea treatment effectively reduces the levels of ubiquitin- and p62-modified proteins, and suppresses inflammatory pathways (Fig. 2e & 3f).

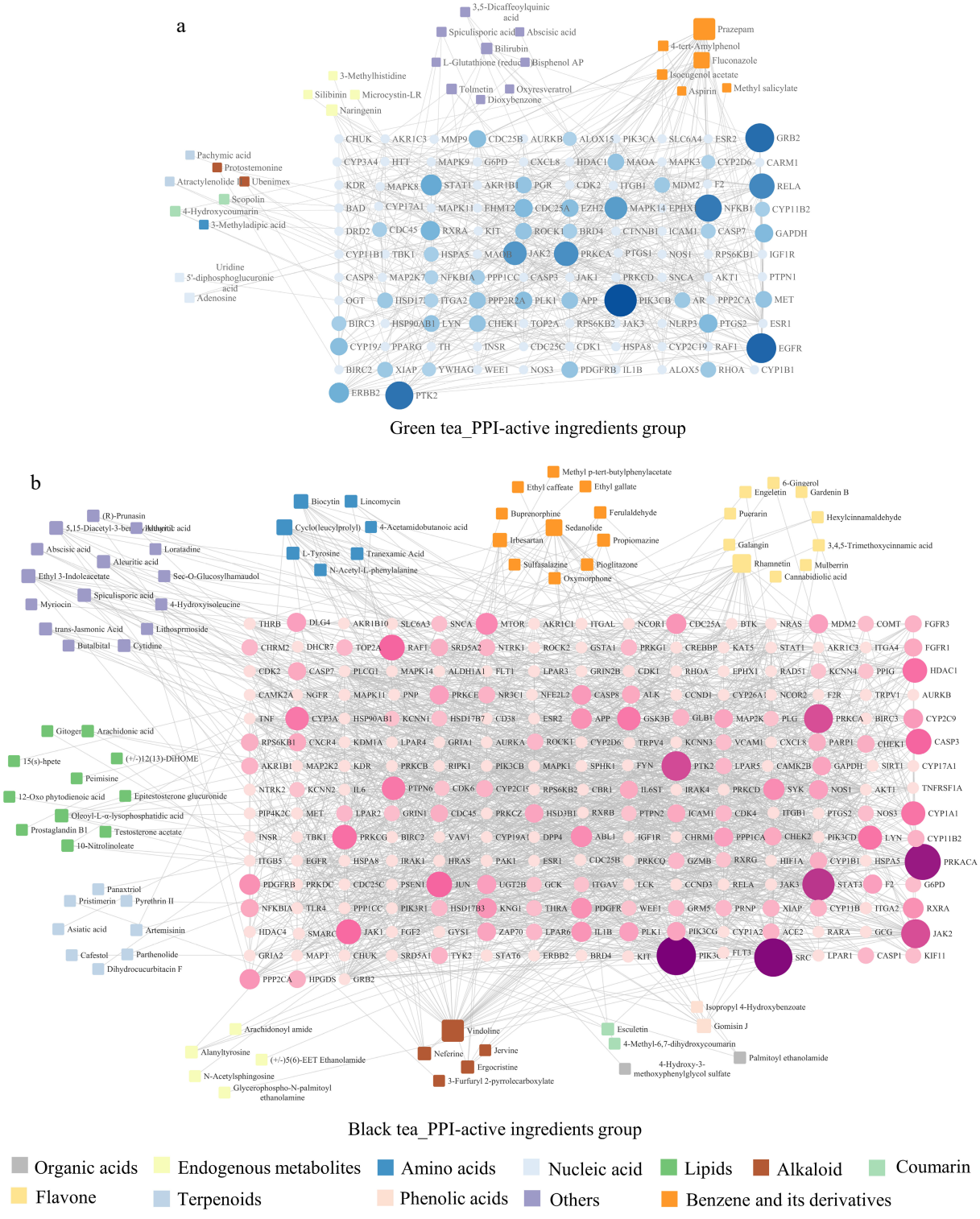

Fig. 6 Network diagram of the active component-key target of green tea and black tea in the intervention of neurodegenerative changes. (a) Association analysis plot for green tea's differential active components with protein-protein interactions (PPI). (b) Similar plot for black tea. Circles in the diagram now represent target genes, with their size and color intensity indicating the extent of their network connections and interaction strength, respectively. Quadrilaterals represent active components, with their size reflecting the degree of linkage to other genes.

Excessive lipid storage is closely associated with metabolic abnormalities[46]. The accumulation of lipids in microglial cells can induced a pro-inflammatory state, hindering the repair mechanisms of the central nervous system. The proper management of lipid storage within cells is crucial for the maintenance of cellular energy balance[47,48]. Black tea has been shown to more effectively reduce the aberrant lipid accumulation induced by Aβ in PC12 cells compared to green tea (Fig. 3h).

Given the prolonged half-lives of proteins in the brain, changes in mRNA translation can have enduring impacts on

neuronal cells and potentially contribute to disease processes[49,50]. The biogenesis of ribosomes, which is critical for both the growth and upkeep of neuronal cells, is compromised under amyloid stress, leading to neuronal atrophy and loss of synaptic connections[49–52]. Hence, targeting the dysregulation in protein synthesis might offer a viable strategy for restoring neuronal functionality. Transcriptome data revealed that black tea counters the disruptions in ribosome-related pathways induced by A$\beta_{25\text{-}35}$. Analysis of DEGs suggested that black tea predominantly enhances axonal growth and signaling pathways, while it diminishes pathways involved in neurodegeneration, translation, and protein folding (Fig. 4e).

Black tea exhibited significant metabolic regulation through the synergistic action of multiple components. The neurodegenerative mechanisms of green tea and black tea were explored using network pharmacology, highlighting how both teas influenced similar signaling pathways. However, the pathways influenced by black tea were characterized by a notably higher count of DEGs (Fig. 5c & d). Analysis of the effective component-target interactions showed that black tea, compared to green tea, contains distinctive components such as organic acids, lipids, phenolic acids, and flavonoids. The metabolic pathways affected by these components are more complex and interconnected (Fig. 6). Notably, the green tea and black tea used in our experiments were derived from the same raw materials harvested in early spring. Differences in the content of common active components like amino acids and caffeine between the two types of tea were minimal, leading to their exclusion from the differential metabolite analysis.

In our investigation, we employed *in vitro* cell models to assess the neuroprotective properties of green tea and black tea, with a focus on *Homo sapien* target genes in network pharmacology analysis. Our findings indicated that black tea impacts a wider array of genes, pointing to a more potent anti-neurodegenerative activity. Nonetheless, these results should be approached with caution. Given the complexity of neurodegenerative conditions and the myriad of bioactive compounds present in tea, further confirmation *via* animal studies is imperative. Future research will extend to *in vivo* experiments to validate the neuroprotective efficacy of black tea and to elucidate its underlying mechanisms more thoroughly. This strategy aims to provide clearer insights into our findings and bolster the evidence supporting black tea's contribution to neuroprotection.

Author contributions

The authors confirm contribution to the paper as follows: methodology, data curation: Wu H, Wan J; investigation, visualization: Yuan J, Xie M, Nie Q; draft manuscript preparation: Wu H, Wan J, Cai S; manuscript review: Cai S; resources: Liu Z; funding acquisition, supervision: Liu Z, Cai S. All authors reviewed the results and approved the final version of the manuscript.

Data availability

Due to administrative requirements, the datasets generated and/or analyzed during this study are not publicly available, but can be obtained from the corresponding author upon reasonable request.

Acknowledgments

This research was funded by the Guangxi Innovation Driven Development Special Fund Project (No. AA20302018), the National Key R&D Program of China (2018YFC1604405), the Key R&D Program of Hunan Province (2020WK2017), National Tea Industry Technology System Research Project of China (CARS-19-C01), National Natural Science Foundation Project of China (31471590, 31100501), and Self-Science Foundation of Hunan Province, China (2019jj50237).

Conflict of interest

The authors declare that they have no conflict of interest. Zhonghua Liu is the Editorial Board member of *Beverage Plant Research* who was blinded from reviewing or making decisions on the manuscript. The article was subject to the journal's standard procedures, with peer-review handled independently of this Editorial Board member and the research groups.

Supplementary Information accompanies this paper at (https://www.maxapress.com/article/doi/10.48130/bpr-0024-0019)

Dates

Received 12 January 2024; Revised 26 March 2024; Accepted 7 April 2024; Published online 20 May 2024

References

1. Opare SKA, Rauk A. 2019. Pseudopeptide designed to inhibit oligomerization and redox chemistry in Alzheimer's disease. *The Journal of Physical Chemistry* 123:5206–15
2. Samanta S, Rajasekhar K, Babagond V, Govindaraju T. 2019. Small molecule inhibits metal-dependent and -independent multifaceted toxicity of Alzheimer's disease. *ACS Chemical Neuroscience* 10:3611–21
3. Chen Z, Zhong C. 2014. Oxidative stress in Alzheimer's disease. *Neurosci Bull* 30:271–81
4. Forloni G, Balducci C. 2018. Alzheimer's disease, oligomers, and inflammation. *Journal of Alzheimer's Disease* 62:1261–76
5. Shoshan-Barmatz V, Nahon-Crystal E, Shteinfer-Kuzmine A, Gupta R. 2018. VDAC1, mitochondrial dysfunction, and Alzheimer's disease. *Pharmacological Research* 131:87–101
6. Naseri NN, Wang H, Guo J, Sharma M, Luo W. 2019. The complexity of tau in Alzheimer's disease. *Neuroscience Letters* 705:183–94
7. Xu T, Niu C, Zhang X, Dong M. 2018. β-Ecdysterone protects SH-SY5Y cells against β-amyloid-induced apoptosis via c-Jun N-terminal kinase- and Akt-associated complementary pathways. *Laboratory Investigation* 98:489–99
8. Neumann U, Ufer M, Jacobson LH, Rouzade-Dominguez ML, Huledal G, et al. 2018. The BACE-1 inhibitor CNP520 for prevention trials in Alzheimer's disease. *EMBO Molecular Medicine* 10:e9316
9. Reiss AB, Arain HA, Stecker MM, Siegart NM, Kasselman LJ. 2018. Amyloid toxicity in Alzheimer's disease. *Reviews in the Neurosciences* 29:613–27
10. Chao AC, Chen CH, Wu MH, Hou BY, Yang DI. 2020. Roles of Id1/HIF-1 and CDK5/HIF-1 in cell cycle reentry induced by amyloid-beta peptide in post-mitotic cortical neuron. *Biochimica et Biophysica Acta - Molecular Cell Research* 1867:118628
11. Caldeira GL, Ferreira IL, Rego AC. 2013. Impaired transcription in Alzheimer's disease: key role in mitochondrial dysfunction and oxidative stress. *Journal of Alzheimer's Disease* 34:115–31

12. Spangenberg EE, Green KN. 2017. Inflammation in Alzheimer's disease: Lessons learned from microglia-depletion models. *Brain, Behavior, and Immunity* 61:1–11
13. Zhou L, Chen D, Huang XM, Long F, Cai H, et al. 2017. Wnt5a promotes cortical neuron survival by inhibiting cell-cycle activation. *Frontiers in Cellular Neuroscience* 11:281
14. Schimidt HL, Garcia A, Martins A, Mello-Carpes PB, Carpes FP. 2017. Green tea supplementation produces better neuroprotective effects than red and black tea in Alzheimer-like rat model. *Food Research International* 100:442–48
15. Hidalgo FJ, Delgado RM, Zamora R. 2017. Protective effect of phenolic compounds on carbonyl-amine reactions produced by lipid-derived reactive carbonyls. *Food Chemistry* 229:388–95
16. Pan SY, Nie Q, Tai HC, Song XL, Tong YF, et al. 2022. Tea and tea drinking: China's outstanding contributions to the mankind. *Chinese Medicine* 17:27
17. Fei T, Fei J, Huang F, Xie T, Xu J, et al. 2017. The anti-aging and anti-oxidation effects of tea water extract in *Caenorhabditis elegans*. *Experimental Gerontology* 97:89–96
18. Pan H, Gao Y, Tu Y. 2016. Mechanisms of Body Weight Reduction by Black Tea Polyphenols. *Molecules* 21:1659
19. Zhao T, Li C, Wang S, Song X. 2022. Green tea (*Camellia sinensis*): a review of its phytochemistry, pharmacology, and toxicology. *Molecules* 27:3909
20. Wang RH, Zhu XF, Qian W, Tang HY, Jiang J, et al. 2018. Effect of tea polyphenols on copper adsorption and manganese release in two variable-charge soils. *Journal of Geochemical Exploration* 190:374–80
21. Deb S, Dutta A, Phukan BC, Manivasagam T, Justin Thenmozhi A, et al. 2019. Neuroprotective attributes of L-theanine, a bioactive amino acid of tea, and its potential role in Parkinson's disease therapeutics. *Neurochemistry International* 129:104478
22. Zhao T, Tang H, Xie L, Zheng Y, Ma Z, et al. 2019. *Scutellaria baicalensis* Georgi. (Lamiaceae): a review of its traditional uses, botany, phytochemistry, pharmacology and toxicology. *Journal of Pharmacy and Pharmacology* 71:1353–69
23. Tanaka T, Matsuo Y. 2020. Production Mechanisms of Black Tea Polyphenols. *Chemical & Pharmaceutical Bulletin* 68:1131–42
24. Li X, Smid SD, Lin J, Gong Z, Chen S, et al. 2019. Neuroprotective and anti-amyloid β effect and main chemical profiles of white tea: comparison against green, oolong and black tea. *Molecules* 24:1926
25. Wan J, Feng M, Pan W, Zheng X, Xie X, et al. 2021. Inhibitory effects of six types of tea on aging and high-fat diet-related amyloid formation activities. *Antioxidants* 10:1513
26. Zheng X, Feng M, Wan J, Shi Y, Xie X, et al. 2021. Anti-damage effect of theaflavin-3'-gallate from black tea on UVB-irradiated HaCaT cells by photoprotection and maintaining cell homeostasis. *Journal of Photochemistry and Photobiology B, Biology* 224:112304
27. Ashraf GM, Greig NH, Khan TA, Hassan I, Tabrez S, et al. 2014. Protein misfolding and aggregation in Alzheimer's disease and type 2 diabetes mellitus. *CNS & Neurological Disorders Drug Targets* 13:1280–93
28. Cai S, Yang H, Zeng K, Zhang J, Zhong N, et al. 2016. EGCG Inhibited Lipofuscin Formation Based on Intercepting Amyloidogenic β-Sheet-Rich Structure Conversion. *PLoS One* 11:e0152064
29. Skene JHP. 1989. Axonal growth-associated proteins. *Annual Review of Neuroscience* 12:127–56
30. Jöbstl E, Fairclough JPA, Davies AP, Williamson MP. 2005. Creaming in black tea. *Journal of Agricultural and Food Chemistry* 53:7997–8002
31. Lim IK. 2006. *TIS21*$^{/BTG2/PC3}$ as a link between ageing and cancer: cell cycle regulator and endogenous cell death molecule. *Journal of Cancer Research and Clinical Oncology* 132:417–26
32. Loreto A, Hill CS, Hewitt VL, Orsomando G, Angeletti C, et al. 2020. Mitochondrial impairment activates the Wallerian pathway through depletion of NMNAT2 leading to SARM1-dependent axon degeneration. *Neurobiology of Disease* 134:104678
33. Cambron M, D'Haeseleer M, Laureys G, Clinckers R, Debruyne J, De Keyser J. 2012. White-matter astrocytes, axonal energy metabolism, and axonal degeneration in multiple sclerosis. *Journal of Cerebral Blood Flow and Metabolism* 32:413–24
34. Chaturvedi RK, Flint Beal M. 2013. Mitochondrial diseases of the brain. *Free Radical Biology & Medicine* 63:1–29
35. Kalia LV, Gingrich JR, Salter MW. 2004. Src in synaptic transmission and plasticity. *Oncogene* 23:8007–16
36. Malm T, Loppi S, Kanninen KM. 2016. Exosomes in Alzheimer's disease. *Neurochemistry International* 97:193–99
37. Lezi E, Swerdlow RH. 2012. Mitochondria in neurodegeneration. *Advances in Experimental Medicine and Biology* 942:269–86
38. Zhao X, Fang J, Li S, Gaur U, Xing X, et al. 2019. Artemisinin attenuated hydrogen peroxide H_2O_2-induced oxidative injury in SH-SY5Y and hippocampal neurons via the activation of AMPK pathway. *International Journal of Molecular Sciences* 20:2680
39. Crouch PJ, Harding SM, White AR, Camakaris J, Bush AI, et al. 2008. Mechanisms of A beta mediated neurodegeneration in Alzheimer's disease. *The International Journal of Biochemistry & Cell Biology* 40:181–98
40. Padmanabhan S, Burke RE. 2018. Induction of axon growth in the adult brain: A new approach to restoration in Parkinson's disease. *Movement Disorders* 33:62–70
41. Yin H, Xu L, Porter NA. 2011. Free radical lipid peroxidation: mechanisms and analysis. *Chemical Reviews* 111:5944–72
42. Orlowski RZ. 1999. The role of the ubiquitin-proteasome pathway in apoptosis. *Cell Death and Differentiation* 6:303–13
43. Kocaturk NM, Gozuacik D. 2018. Crosstalk Between Mammalian Autophagy and the Ubiquitin-Proteasome System. *Frontiers in Cell and Developmental Biology* 6:128
44. Martin-Rincon M, Pérez-López A, Morales-Alamo D, Perez-Suarez I, de Pablos-Velasco P, et al. 2019. Exercise mitigates the loss of muscle mass by attenuating the activation of autophagy during severe energy deficit. *Nutrients* 11:2824
45. Zaffagnini G, Savova A, Danieli A, Romanov J, Tremel S, et al. 2018. p62 filaments capture and present ubiquitinated cargos for autophagy. *The EMBO Journal* 37:e98308
46. Daemen S, van Zandvoort MAMJ, Parekh SH, Hesselink MKC. 2016. Microscopy tools for the investigation of intracellular lipid storage and dynamics. *Molecular Metabolism* 5:153–63
47. Loix M, Wouters E, Vanherle S, Dehairs J, McManaman JL, et al. 2022. Perilipin-2 limits remyelination by preventing lipid droplet degradation. *Cellular and Molecular Life Sciences* 79:515
48. Veliova M, Petcherski A, Liesa M, Shirihai OS. 2020. The biology of lipid droplet-bound mitochondria. *Seminars in Cell & Developmental Biology* 108:55–64
49. Moreno JA, Radford H, Peretti D, Steinert JR, Verity N, et al. 2012. Sustained translational repression by eIF2α-P mediates prion neurodegeneration. *Nature* 485:507–11
50. Jishi A, Qi X, Miranda HC. 2021. Implications of mRNA translation dysregulation for neurological disorders. *Seminars in Cell & Developmental Biology* 114:11–19
51. Meier S, Bell M, Lyons DN, Rodriguez-Rivera J, Ingram A, et al. 2016. Pathological tau promotes neuronal damage by impairing ribosomal function and decreasing protein synthesis. *The Journal of Neuroscience* 36:1001–7
52. Stein KC, Morales-Polanco F, van der Lienden J, Rainbolt TK, Frydman J. 2022. Ageing exacerbates ribosome pausing to disrupt cotranslational proteostasis. *Nature* 601:637–42